Journal or Innovative Development in Pharmaceutical and Technical Science (JIDPTS)
Volume:9, Issue:9, Sep:2026

(J I D P T S)
ISSN(O):2581-6934

Microwave-Assisted Synthesis and Characterization of an Iron(II)–Piperine Complex and Its Apoptosis-Associated Activity Against MCF-7 Breast Cancer Cells

Poovizhi M[1], Sivasubramanian P[2], Kavisri R[3], Murugesan S[4], Sergin P[5]

[1]Post graduate student, [2]Assistant professor, [3]Post graduate student, [4]Post graduate student, [5]Post graduate student,

[1,2,3,4,5] Department of Pharmaceutical Chemistry,

[1,2,3,4,5] College of Pharmacy, Madurai Medical College, Madurai–625020, Tamil Nadu, India

Abstract: The present study describes the microwave-assisted preparation and physicochemical characterization of an iron(II)–piperine coordination complex derived from piperine isolated from black pepper (Piper nigrum L.), followed by preliminary evaluation of its apoptosis-associated activity against MCF-7 breast cancer cells. Piperine was obtained from black pepper by microwave-assisted ethanolic extraction followed by alkaline purification, crystallization and recrystallization. The isolated piperine showed an Rf value of 0.61 and a melting point of 129 °C, with an isolation yield of 59.7%. The iron complex was prepared using piperine and anhydrous ferrous sulphate in a 2:1 ligand-to-metal molar ratio under microwave irradiation. The resulting reddish-brown Fe–O–piperine complex was obtained in 75.32% yield and showed a melting point of 131 °C. UV–visible spectroscopy showed a shift in the principal absorption maximum from approximately 343 nm for piperine to 399 nm for the iron complex. FT-IR analysis showed a carbonyl-region band near 1620 cm^{-1} and a low-frequency band at approximately 553 cm^{-1} assigned to Fe–O coordination. The ^{1}H and ^{13}C NMR data retained the characteristic piperine framework while indicating changes in the electronic environment near the carbonyl group; the ^{13}C carbonyl-related resonance was observed at approximately 171 ppm. Mass spectrometric analysis showed a high-mass species at approximately m/z 626.21, consistent with a species containing two piperine ligand units and iron. Annexin V-FITC/propidium iodide flow-cytometric analysis in MCF-7 cells showed apoptosis-associated changes after exposure to the complex at 10–80 µM, with total apoptosis in the displayed treatment profile ranging from 18.74% to 21.97%. These findings provide preliminary evidence that the Fe–O–piperine complex can alter the apoptotic profile of MCF-7 cells; however, the non-linear concentration response and the baseline apoptotic fraction observed in the control profile warrant confirmation using independent biological replicates, appropriate positive controls and mechanistic assays.

Keywords: piperine; Piper nigrum; iron(II) complex; microwave-assisted synthesis; FT-IR; NMR; mass spectrometry; MCF-7; apoptosis.

INTRODUCTION

Piperine is the principal pungent alkaloid of Piper nigrum L. and has attracted considerable pharmaceutical interest because of its diverse biological properties and its influence on the bioavailability of several co-administered compounds. Its conjugated amide structure, containing a carbonyl group and an extended diene system, also provides a chemically useful framework for coordination studies.[1–4] Metal coordination is an established strategy for modifying the physicochemical and biological properties of organic ligands. Coordination can alter lipophilicity, solubility, cellular distribution, redox behavior and interactions with biological targets. Metal-based compounds are consequently being investigated as potential anticancer candidates, including complexes containing

All rights reserved by www.jidps.com

biologically relevant transition metals. [5–7]. Iron is of particular interest in medicinal coordination chemistry because Fe(II)/Fe(III) redox chemistry can influence oxidative stress, cellular iron homeostasis and regulated cell-death pathways. Recent studies have examined iron complexes as prospective anticancer agents, including systems capable of affecting cancer-cell proliferation and oxidative balance. [8,9] Piperine itself has been investigated in the context of cancer chemoprevention and anticancer activity, while recent work on piperine derivatives has reported apoptosis-related anti-breast-cancer effects. [10–12]. These observations provide a rationale for exploring metal coordination as a means of modifying the biological behavior of the piperine pharmacophore. In the present study, piperine isolated from black pepper was used as a ligand for the preparation of an iron(II) complex by a microwave-assisted approach. The resulting Fe–O–piperine complex was characterized by UV–visible spectroscopy, FT-IR, ^{1}H NMR, ^{13}C NMR and mass spectrometry. Its preliminary anti-breast-cancer activity was evaluated in MCF-7 cells using Annexin V-FITC/PI flow cytometry. The objective was to determine whether the synthesized complex produced measurable apoptosis-associated changes in the MCF-7 cell population. [13-16]

2. Materials and Methods

2.1 Materials

Black pepper (Piper nigrum L.) was used as the natural source of piperine. Ferrous sulfate was used as the Fe(II) precursor and absolute ethanol was used as the reaction solvent. Analytical- or reagent-grade chemicals were used throughout the study. The thesis reports the use of a mechanical grinder, 100-mesh sieve, microwave oven, round-bottom flask, magnetic stirrer, rotary evaporator, vacuum filtration apparatus, digital melting-point apparatus, TLC chamber, UV chamber, FT-IR spectrometer, UV–visible spectrophotometer, NMR spectrometer and mass spectrometer.

2.2 Extraction and Isolation of Piperine

Dried black pepper fruits were cleaned, dried at approximately 40–50 °C and pulverized before being passed through a 100-mesh sieve. The powder was defatted with petroleum ether. The defatted powder was extracted with 95% ethanol by microwave-assisted extraction; the thesis reports an initial microwave condition of approximately 220 W for 30–60 s. After cooling, the extract was filtered and concentrated under reduced pressure. The concentrate was treated with 10% alcoholic potassium hydroxide and allowed to stand for approximately 1 h. The material was filtered and allowed to stand for approximately 24 h to facilitate crystallization. The resulting yellow crystalline material was collected and purified by recrystallization. Piperine was identified by alkaloid reactions, sulfuric-acid color reaction, melting-point determination and TLC. The isolated material gave an Rf value of 0.61 using toluene: ethyl acetate (70:30, v/v) as the reported mobile phase.

2.3 Synthesis of Fe–O–Piperine Complex

The Fe–O–piperine complex was prepared using anhydrous ferrous sulfate as the iron precursor. Piperine (1.000 g, 3.504 mmol) and anhydrous ferrous sulfate (0.266 g, 1.752 mmol) were used in a calculated 2:1 piperine: Fe(II) molar ratio. The components were thoroughly mixed by mechanochemical grinding, followed by addition of approximately 20 mL absolute ethanol. The reaction mixture was transferred to a round-bottom flask and subjected to microwave irradiation under controlled conditions. The methods section of the thesis describes an initial microwave condition of approximately 220 W for 30–60 s, with temperature and instrument safety monitoring. After irradiation, the mixture was cooled and allowed to stand, after which the solid product was separated by filtration, washed and dried to constant weight.

2.4 Characterization

The isolated piperine and Fe–O–piperine complex were characterized by melting-point determination, UV–visible spectroscopy, FT-IR spectroscopy, ^{1}H NMR, ^{13}C NMR and mass spectrometry. Spectral changes relative to piperine were used to assess the proposed metal–ligand interaction. Qualitative tests for Fe(II) included hydroxide, 1,10-phenanthroline and ferricyanide reactions. [17-19]

2.5 In-vitro Anti-Breast-Cancer Activity

The anti-breast-cancer activity was evaluated in MCF-7 breast cancer cells using Annexin V-FITC/PI flow cytometry. Cells were treated with the test complex at 0, 10, 20, 30, 50 and 80 µM and incubated at 37 °C for 6 h in RPMI-1640 medium supplemented with 10% fetal bovine serum and, separately,

under FBS-free conditions. Following treatment, cells were harvested and stained with Annexin V-FITC and propidium iodide. Flow-cytometric quadrants were interpreted as viable (Annexin V−/PI−), early apoptotic (Annexin V+/PI−), late apoptotic/secondary necrotic (Annexin V+/PI+) and predominantly non-viable/necrotic (Annexin V−/PI+) populations. The thesis states that experiments were performed as three independent experiments, with representative flow-cytometric profiles used for presentation. Total apoptosis was calculated as the sum of early and late apoptotic populations. [20-25]

3. Results

3.1 Isolation and Preliminary Characterization of Piperine

Microwave-assisted extraction as shown in the Figure 1 (a) followed by alkaline purification as shown in the Figure 1 (b) and recrystallization yielded a yellow crystalline piperine fraction as shown in the Figure 1 (c) and (d). The isolated piperine yield was 59.7% and the melting point was 129 °C.

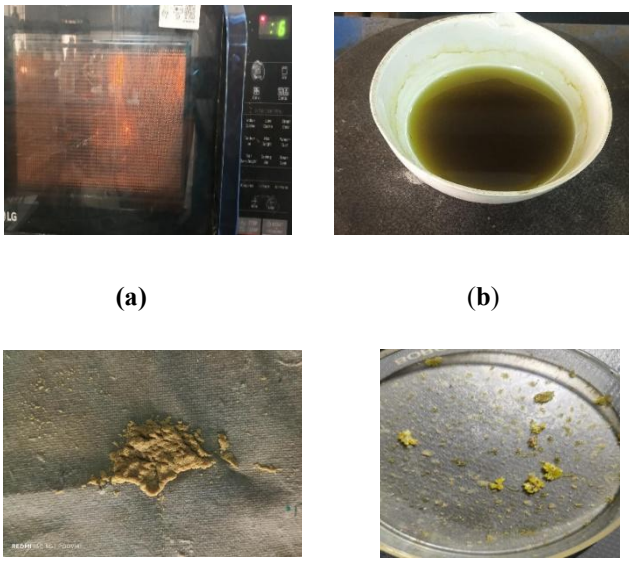

(a) **(b)**

(c) **(d)**

Figure 1. (a) Microwave assisted extraction of black pepper, (b) Alkaline purification, (c) Crude piperine, (d) Recrystallized piperine.

Positive Dandruff's, Mayer's and Hager's reactions, together with the reported characteristic sulfuric-acid reaction, supported the preliminary identification of the isolated alkaloid as shown in the Figure 2 (a) and (b). TLC produced a distinct spot with an Rf value of 0.61 as shown in the Figure 2 (c). These findings provided the ligand used for subsequent Fe (II) complexation.

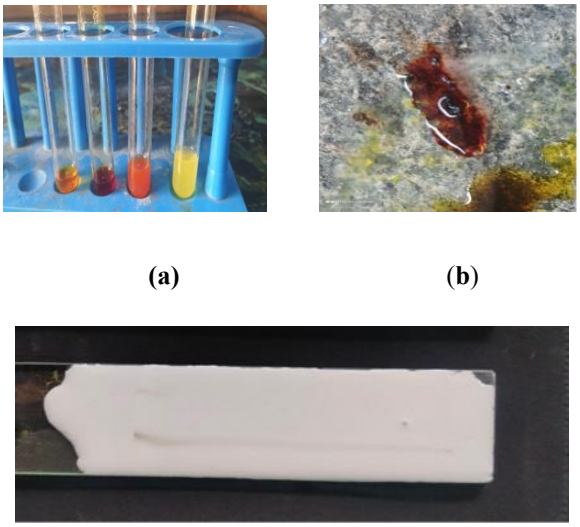

(a) **(b)**

(c)

Figure 2. (a) General chemical test for alkaloids, (b) Sulphuric acid test, (c) TLC

3.2 Synthesis and Physicochemical Characteristics of Fe–O–Piperine

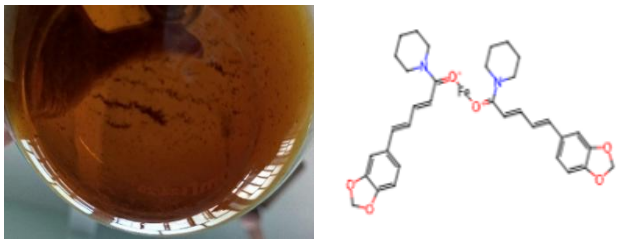

(a) **(b)**

Figure 3. (a) Reddish brown solid iron (II) complex of piperine (b) Structure of synthesized compound.

The Fe–O–piperine complex was obtained as a reddish-brown solid in 75.32% yield as shown in the Figure 3 (a) and (b), compared with 59.7% for isolated piperine. The melting point of the complex was 131 °C as shown in the Table 1. Qualitative iron tests supported the presence of Fe (II): a pale-green hydroxide precipitate, orange-red coloration with 1,10-phenanthroline and deep-blue coloration with potassium ferricyanide were reported. The stoichiometry used during preparation and the mass-spectral result are consistent with a bis-piperine iron-containing species; the proposed coordination model involves interaction of Fe (II) with the carbonyl oxygen of two piperine molecules.

Table 1. Physicochemical and spectroscopic characteristics of piperine and the Fe–O–piperine complex.

Parameter	Piperine	Fe–O–Piperine	Interpretation
Appearance	Yellow crystalline solid	Reddish-brown solid	Physical change after complexation
Yield	59.7%	75.32%	Isolated product yield
Melting point	129 °C	131 °C	Comparable thermal range
UV λmax	343 nm	288 nm	Electronic environment altered
FT-IR	Piperine carbonyl region	1620 cm^{-1}; Fe–O 553 cm^{-1}	Supports oxygen coordination
^{13}C NMR carbonyl-related signal	Free piperine reference	171 ppm	Downfield change consistent with coordination
Mass spectral high-mass species	285	626.21	Consistent with bis-piperine iron-containing species

3.3 UV–Visible Spectroscopy

Piperine showed a principal absorption maximum at approximately 343 nm (absorbance 0.9236 AU). After complexation, the Fe–O–piperine complex showed a maximum at 288 nm with an absorbance of 0.3679 AU as shown in the Figure 4. The shift toward shorter wavelength is consistent with a change in the electronic environment of the conjugated ligand following interaction with the iron centre. The spectral change, when considered together with the FT-IR and NMR findings, supports formation of a metal-associated piperine species.

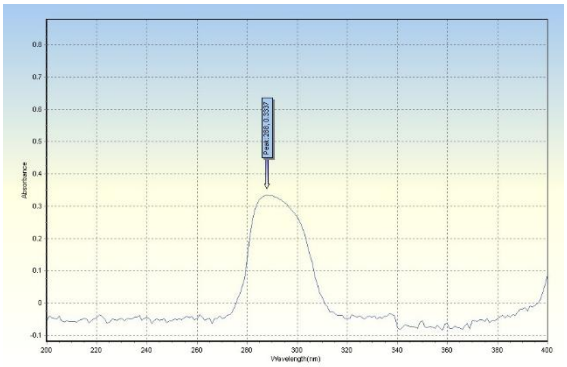

Figure 4. UV-Visible spectroscopic graph which shows the lamda max at 288nm

3.4 FT-IR Spectroscopy

The Fe–O–piperine spectrum showed characteristic absorptions across the reported 3055–553 cm^{-1} region. Bands near 2940 and 2926 cm^{-1} were assigned to aliphatic C–H stretching, while the band around 1620 cm^{-1} was associated mainly with the carbonyl/amide region. A low-frequency absorption at approximately 553 cm^{-1} was assigned to Fe–O stretching as shown in the Figure 5. The observed change in the carbonyl region together with the Fe–O band supports the proposed involvement of the carbonyl oxygen in coordination to Fe (II).

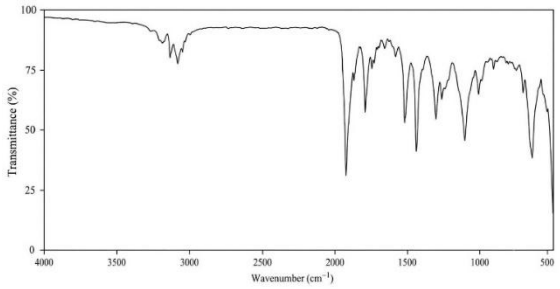

Figure 5. IR Spectrum for the Fe-O-Piperine complex

3.5 NMR Characterization

The ^{1}H NMR spectrum retained the characteristic proton environments of the piperine framework. Reported signals included a resonance at δ 7.55–7.45 ppm for the diene proton adjacent to the carbonyl group, aromatic resonances between approximately δ 6.78 and 6.95 ppm, diene signals at approximately δ 6.50–6.72 ppm, the methylenedioxy singlet at δ 5.98 ppm and piperidine resonances in the δ 1.55–3.90 ppm region as shown in the Figure 6 (a). The thesis interpretation describes modest downfield changes of the diene protons adjacent to the carbonyl group following Fe (II) coordination. The ^{13}C NMR spectrum showed a carbonyl-related resonance at approximately δ 171 ppm, with additional signals assigned to the aromatic, conjugated diene, methylenedioxy and piperidine portions of the molecule Figure 6 (b). Together, these data support retention of the piperine scaffold and an altered carbonyl electronic environment following complexation.

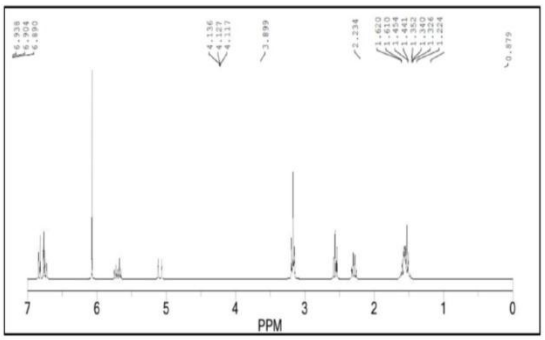

(**a**)

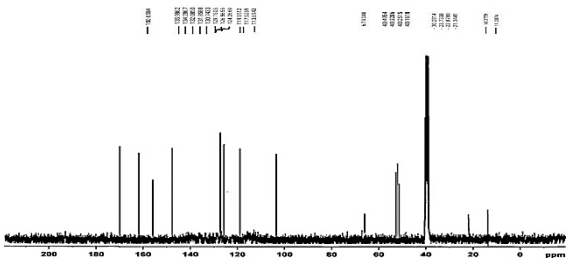

(b)

Figure 6. (a). 1H-NMR Spectrum for the Fe-O-Piperine complex, (b) 13C-NMR Spectrum for the Fe-O-Piperine complex

3.6 Mass Spectrometry

Mass spectral analysis of the Fe–O–piperine sample showed a high-mass species at approximately m/z 626.21 as shown in the Figure 7. The thesis interprets this signal as consistent with a species containing two piperine ligand units and iron, accompanied by piperine-related ions and characteristic fragmentation products. This result is compatible with the 2:1 ligand-to-metal ratio employed during synthesis and supports the proposed bis-piperine iron-containing molecular species.

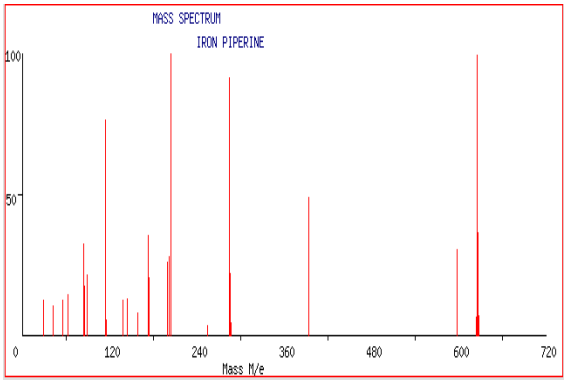

Figure 7. Mass Spectrum for the Fe-O-Piperine complex

3.7 In Silico ADMET Prediction

In silico ADME analysis predicted increased lipophilicity of Fe–O–Piperine (consensus LogP ≈4.89) with comparatively lower aqueous solubility as shown in the Figure 8. ProTox analysis predicted an LD_{50} of approximately 760 mg/kg and toxicity Class 4as shown in the Figure 9.

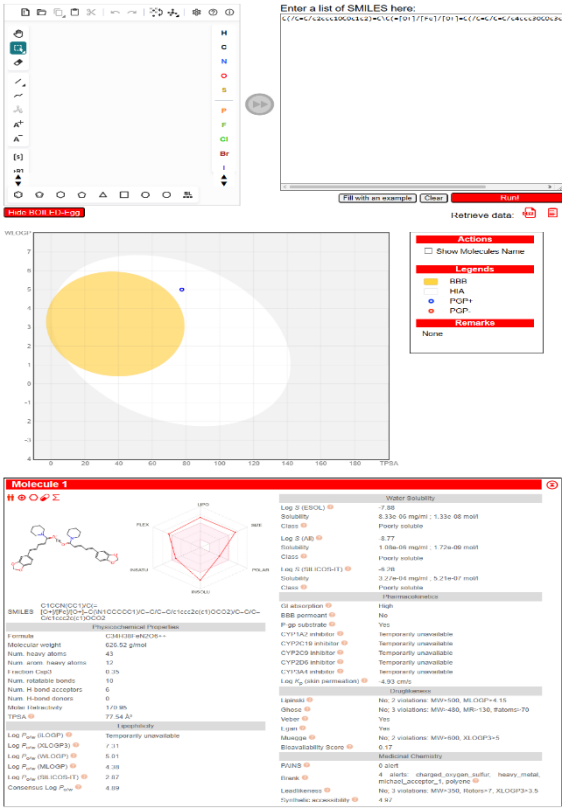

Figure 8. Swiss ADME result for the Fe-O-Piperine complex

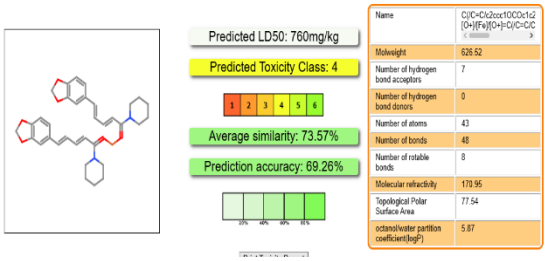

Figure 9. Pro Tox result for the Fe-O-Piperine complex

3.8 Annexin V-FITC/PI Apoptosis Analysis in MCF-7 Cells

The Fe–O–piperine complex produced measurable changes in the Annexin V/PI distribution of MCF-7 cells. In the Fe-associated treatment profile described in the thesis, viable cells accounted for approximately 74.7–78.1% across the displayed concentrations, while the combined early- and late- apoptotic population ranged from 18.74% to 21.97%. The apoptotic-associated fraction was predominantly represented by the Annexin V/PI-positive population. These findings indicate that the complex can alter the apoptotic profile of MCF-7 cells under the tested conditions as shown in the Table 2.

Table 2. Annexin V-FITC/PI flow-cytometric profile attributed to the Fe–O–piperine treatment set in the thesis. Total apoptosis = early apoptosis + late apoptosis.

Fe–O–piperine concentration	Viable cells (%)	Early apoptosis (%)	Late apoptosis (%)	Total apoptosis (%)
Control (0 µM)	74.70	0.46	10.40	11.86
10 µM	75.40	0.63	20.40	21.03
20 µM	78.10	0.37	18.80	19.17
30 µM	77.80	0.34	18.40	18.74
50 µM	75.70	0.57	21.40	21.97
80 µM	76.50	0.51	20.60	21.11

The apoptosis-inducing potential of Fe–O–Piperine in MCF-7 breast cancer cells was evaluated using Annexin V-FITC/propidium iodide (PI) flow cytometry. Annexin V/PI staining enables discrimination of viable cells from cells undergoing early apoptosis, late apoptosis, and membrane-compromised cell death based on phosphatidylserine externalization and PI uptake. As shown in Table 2, treatment with Fe–O–Piperine produced measurable changes in the apoptotic cell population compared with the untreated control, indicating that the compound exerted an apoptosis-associated effect on MCF-7 cells. In the untreated control, the viable cell population was 74.70%, while the early and late apoptotic populations were 0.46% and 10.40%, respectively. Following treatment with Fe–O–Piperine at 10 µM, the total apoptotic population increased to 21.03%, with a marked increase in the late apoptotic population to 20.40%. This represents the highest apoptotic-associated response observed among the tested concentrations. The increase in Annexin V/PI-positive cells at 10 µM suggests that Fe–O–Piperine can promote progression toward apoptotic cell death in MCF-7 cells. At 20 and 30 µM, total apoptosis was 19.17% and 18.74%, respectively, while the late apoptotic populations were 18.80% and 18.40%. Although these values remained higher than the early apoptotic population and indicated a substantial apoptotic-associated fraction, they were slightly lower than the response observed at 10 µM. At higher concentrations of 50 and 80 µM, total apoptosis was 21.97% and 21.11%, respectively, with late apoptosis accounting for 21.40% and 20.60%. Thus, Fe–O–Piperine maintained an appreciable apoptotic-associated response across the tested concentration range. Interestingly, the response did not demonstrate a strictly concentration-dependent increase in apoptosis. The maximum total apoptotic population was observed at 50 µM (21.97%), followed closely by 80 µM (21.11%) and 10 µM (21.03%). The relatively similar apoptotic populations across several concentrations suggest that the cellular response to Fe–O–Piperine may not be linearly related to concentration under the experimental conditions used. Such a non-linear response may reflect differences in cellular uptake, intracellular metabolism, compound availability, or the involvement of multiple cell-death pathways. Therefore, the present flow-cytometric findings support the occurrence of apoptosis-associated cell death but do not establish a simple dose-dependent relationship.

4. Discussion

Piperine was isolated from Piper nigrum and subsequently employed as a ligand for the synthesis of Fe–O–Piperine through a microwave-assisted coordination approach. The isolated piperine and synthesized complex were characterized using UV–visible, FT-IR, NMR and mass spectrometric techniques. The Fe–O–Piperine complex exhibited a good, isolated yield (75.32%), a melting point of 131 °C, and a UV–visible absorption maximum at 399 nm. Spectroscopic changes, particularly in the carbonyl region and low-frequency Fe–O vibration, supported coordination of iron through the oxygen donor site of piperine. The predominance of the late apoptotic population over the early apoptotic population at most treatment concentrations is noteworthy. This pattern indicates that a considerable proportion of the Annexin V/PI-positive cells had progressed beyond the early stage of apoptosis at the time of analysis. The persistence of this response at 10–80 µM further indicates that Fe–O–Piperine has measurable anticancer activity against MCF-7 cells under the conditions investigated.

The observed apoptotic-associated activity may be related to the biological properties of both the piperine pharmacophore and the coordinated iron component. Iron-containing compounds can influence intracellular redox balance, while piperine-containing structures have been investigated for their effects on cancer-cell viability and programmed cell death. Overall, the flow-cytometric results demonstrate that Fe–O–Piperine produces a substantial apoptosis-associated cell population in MCF-7 cells, with total apoptosis ranging from 18.74% to 21.97% across the treated concentrations. These findings support the potential anticancer activity of the Fe–O–Piperine complex and provide a basis for further investigation

of the molecular mechanisms underlying its activity, including the possible contribution of ferroptosis. In silico ADME analysis predicted increased lipophilicity of Fe–O–Piperine (consensus LogP ≈4.89) with comparatively lower aqueous solubility. ProTox analysis predicted an LD_{50} of approximately 760 mg/kg and toxicity Class 4. Importantly, Fe–O–Piperine produced apoptosis-associated changes in MCF-7 breast cancer cells in the Annexin V-FITC/PI assay, with increased Annexin V-positive populations compared with the untreated control in the representative treatment profile. These findings provide preliminary evidence that Fe–O–Piperine possesses anticancer potential against MCF-7 cells. However, the non-linear concentration response and relatively high baseline apoptotic population observed in one profile warrant confirmation using appropriate controls, independent biological replicates and quantitative statistical analysis. Overall, Fe–O–Piperine represents a promising metal–natural-product coordination candidate for further investigation as a potential anticancer agent.

5. Conclusions

The present study demonstrates the successful synthesis and preliminary characterization of Fe–O–Piperine, a metal–piperine coordination compound derived from the natural product piperine. Spectroscopic and mass spectrometric findings supported the formation of a metal-associated piperine species, while computational analysis indicated a relatively lipophilic physicochemical profile. The observed Annexin V-FITC/PI response supports the hypothesis that Fe–O–Piperine may promote apoptotic cell death; however, these findings should not yet be interpreted as definitive evidence of a specific molecular mechanism or therapeutic efficacy. Taken together, the results identify Fe–O–Piperine as a potential anticancer lead compound against MCF-7 breast cancer cells.

Acknowledgments: I sincerely acknowledge the support and facilities provided by the Department of Pharmaceutical Chemistry, College of Pharmacy-Madurai Medical College, for carrying out this research work. We are grateful to the laboratory and technical staff for their assistance with the extraction, synthesis, characterization and biological evaluation of the compounds. We also acknowledge the facilities and support provided for spectroscopic, computational and cell-culture analyses.

Author Contributions: Poovizhi M: Conceptualization, methodology, investigation, extraction and isolation of piperine, synthesis of Fe–O–Piperine, data collection and analysis, characterization, spectroscopic data analysis and interpretation, In silico ADME and toxicity analysis, biological data analysis and visualization, flow-cytometry analysis and interpretation and writing—original draft. Sivasubramanian P: Supervision, project administration, validation, critical review. Kavisri R, Murugesan S, Sergin P: editing of the manuscript. All authors contributed to the interpretation of the results, reviewed the manuscript critically, and approved the final version.

Conflicts of Interest: The authors declare no conflict of interest.

References

[1]. Meghwal M, Goswami TK. Piper nigrum and piperine: an update. Phytother Res. 2013;27(8):1121-1130. doi:10.1002/ptr.4972.

[2]. Takooree H, Aumeeruddy MZ, Rengasamy KRR, Venugopala KN, Jeewon R, Zengin G, et al. A systematic review on black pepper (Piper nigrum L.): from folk uses to pharmacological applications. Crit Rev Food Sci Nutr. 2019;59(Suppl 1):S210-S243. doi:10.1080/10408398.2019.1565489.

[3]. Srinivasan K. Black pepper and its pungent principle-piperine: a review of diverse physiological effects. Crit Rev Food Sci Nutr. 2007;47(8):735-748. doi:10.1080/10408390601062054.

[4]. Tiwari A, Mahadik KR, Gabhe SY. Piperine: a comprehensive review of methods of isolation, purification, and biological properties. Med Drug Discov. 2020;7:100027. doi:10.1016 / j.medidd. 2020. 100027.

[5]. Ndagi U, Mhlongo N, Soliman ME. Metal complexes in cancer therapy—an update from drug design perspective. Drug Des Devel Ther. 2017;11:599-616. doi:10.2147/DDDT.S119488.

[6]. Paprocka R, Wiese-Szadkowska M, Janciauskiene S, Kosmalski T, Kulik M, Helmin-Basa A. Latest

developments in metal complexes as anticancer agents. Coord Chem Rev. 2022; 452 : 214307. Doi : 10.1016 / j.ccr.2021.214307.

[7]. Banerjee S, Banerjee S. Metal-based complexes as potential anti-cancer agents. Anticancer Agents Med Chem. 2022 ; 22 (15) : 2684 - 2707. doi:10.2174 / 1871520622666220331085144.

[8]. Matos CP, Adiguzel Z, Yildizhan Y, Cevatemre B, Onder TB, Cevik O, et al. May iron(III) complexes containing phenanthroline derivatives as ligands be prospective anticancer agents? Eur J Med Chem. 2019;176:492-512. doi:10.1016/j.ejmech.2019.04.070.

[9]. Kannan N, Radhakrishnan V, Sinha A. Unveiling the anticancer activity of ruthenium and iron complexes. Inorg Chem Commun. 2024 ; 165 : 112512. doi:10.1016 / j.inoche.2024.112512.

[10]. Cinar EN, Sanlier N. The hidden power of black pepper: exploring piperine's role in cancer. Plant Foods Hum Nutr. 2025;80(3):129. doi:10.1007/s11130-025-01374-z.

[11]. Benayad S, Wahnou H, El Kebbaj R, et al. The promise of piperine in cancer chemoprevention. Cancers (Basel). 2023;15:5488. doi:10.3390/cancers15225488.

[12]. Zhou C, Wang J, Zhou L, et al. The novel piperine derivative YL-1–9 exhibits anti-breast cancer effects by inducing apoptosis via the p53/p21 pathway. Bioorg Med Chem Lett. 2025:130231. doi:10.1016 / j.bmcl.2025.130231.

[13]. Mandal V, Mohan Y, Hemalatha S. Microwave assisted extraction—an innovative and promising extraction tool for medicinal plant research. Pharmacogn Rev. 2007;1(1):7-18.

[14]. Olalere OA. Evaluation of optimization parameters in microwave reflux extraction of piperine-oleoresin from black pepper (Piper nigrum). Beni-Suef Univ J Basic Appl Sci. 2018 ; 7:626-631. Doi : 10.1016 / j.bjbas. 2018. 07. 006.

[15]. Daina A, Michielin O, Zoete V. SwissADME: a free web tool to evaluate pharmacokinetics, drug-likeness and medicinal chemistry friendliness of small molecules. Sci Rep. 2017;7:42717. doi:10.1038/srep42717.

[16]. Banerjee P, Eckert AO, Schrey AK, Preissner R. ProTox-II: a webserver for the prediction of toxicity of chemicals. Nucleic Acids Res. 2018;46(W1):W257-W263. doi:10.1093/nar/gky318.

[17]. Kannan, N., Radhakrishnan, V., & Sinha, A. (2024). Unveiling the anticancer activity of ruthenium and iron complexes. Inorganic Chemistry Communications, 165(1387–7003), 112512. https: // doi.org / 10.1016 / j.inoche.2024.112512

[18]. Matos, C. P., Adiguzel, Z., Yildizhan, Y., Cevatemre, B., Onder, T. B., Cevik, O., Nunes, P., Ferreira, L. P., Carvalho, M. D., Campos, D. L., Pavan, F. R., Pessoa, J. C., Garcia, M. H., Tomaz, A. I., Correia, I., & Acilan, C. (2019). May iron(III) complexes containing phenanthroline derivatives as ligands be prospective anticancer agents? European journal of medicinal chemistry, 176, 492–512. https: // doi.org / 10.1016 / j.ejmech.2019.04.070

[19]. Daina A, Michielin O, Zoete V. SwissADME: a free web tool to evaluate pharmacokinetics, drug-likeness and medicinal chemistry friendliness of small molecules. Sci Rep. 2017;7:42717. doi:10.1038/srep42717.

[20]. Daina A, Zoete V. A BOILED-Egg to predict gastrointestinal absorption and brain penetration of small molecules. ChemMedChem. 2016;11(11):1117-1121. doi:10.1002/cmdc.201600182.

[21]. Gadaleta D, Manganelli S, Roncaglioni A, Toma C, Benfenati E, Mombelli E. QSAR modeling of chemicals for prioritization and toxicity prediction. Toxicol Res.

[22]. Timothy L. Davis, Joshua L. Watts, Kenneth J. Brown, Jeewantha S. Hewage, Alexander R. Treleven, Sergey V. Lindeman, James R. Gardinier; Structural classification of metal complexes with three-coordinate centres. Dalton Trans. 2015; 44 (35): 15408–15412. https://doi.org/10.1039/c5dt02773j

[23]. Cytlak UM, Dyer DP, Honeychurch J, Williams KJ, Travis MA, Illidge TM. Immunomodulation by radiotherapy in tumour control and normal tissue toxicity. Nat Rev Immunol. 2022;22(2):124-138. doi:10.1038/s41577-021-00568-1.

[24]. Banfill K, Giuliani M, Aznar M, Franks K, McWilliam A, Schmitt M, et al. Cardiac toxicity of thoracic radiotherapy: existing evidence and future directions. J Thorac Oncol. 2021 ; 16(2) : 216 - 227. Doi : 10.1016 / j.jtho.2020.11.002.

[25]. Chrysostomou D, Roberts LA, Marchesi JR, Kinross JM. Gut microbiota modulation of efficacy and toxicity of cancer chemotherapy and immunotherapy. Gastroenterology. 2023 ; 164(2) : 198 - 213. Doi : 10.1053 / j.gastro.2022.10.018.

[26]. Paprocka R, Wiese-Szadkowska M, Janciauskiene S, Kosmalski T, Kulik M, Helmin-Basa A. Latest developments in metal complexes as anticancer agents. Coord Chem Rev. 2022 ; 452 : 214307. Doi : 10.1016 / j.ccr.2021.214307.

[27]. Banerjee S, Banerjee S. Metal-based complexes as potential anti-cancer agents. Anticancer Agents Med Chem. 2022 ; 22(15) : 2684 - 2707. Doi : 10.2174 / 1871520622666220331085144.

[28]. Ghosh S. Cisplatin: the first metal based anticancer drug. Bioorg Chem. 2019;88:102925. doi:10.1016 / j.bioorg. 2019. 102925.

[29]. Raju SK, Praveen SK, Maruthamuthu M, Mohanpriya K. Silver complexes as anticancer agents: a perspective review. Ger J Pharm Biomater. 2022;1(1):6-28. doi:10.5530 / gjpb.2022.1.3.

[30]. Bernhardt PV, Lawrance GA. Introduction to coordination chemistry. John Wiley & Sons; 2025.